Soft Matter

View Online
Dynamic Article Links

Cite this: DOI: 10.1039/c1sm05954h

www.rsc.org/softmatter

COMMUNICATION

Phonon-like excitation in secondary and tertiary structure of hydrated protein powders

Mingda Li,[a] Xiang-qiang Chu,[a] Emiliano Fratini,[b] Piero Baglioni,[b] Ahmet Alatas,[c] E. Ercan Alp[c] and Sow-Hsin Chen*[a]

Received 23rd May 2011, Accepted 8th August 2011
DOI: 10.1039/c1sm05954h

Existence of sub-thermal collective excitations in proteins is of great interest due to its possible close coupling with the onset of their biological functions. We use high-energy resolution inelastic X-ray scattering to directly measure phonon dispersion relations and their damping in two hydrated proteins, α-chymotrypsinogen A and casein, differing in their secondary and tertiary structures. We observe that specific phonons in the Q range 28–30 nm^{-1} are markedly softened only above T_D = 220 K, the observed protein dynamic transition temperature. This might indicate that only phonon modes within the wavelengths in the length scale comparable to the secondary structure dimension could be linked to the onset of protein biological activity. We also infer that the presence of tertiary structure contributes little to the population of phonons, while the α-helix seems to be the major contributor to phonons propagation.

A phonon of a characteristic wave number Q (magnitude of the wave vector transfer $\vec{Q}$) is the collective density oscillation of a well-defined wavelength $\lambda = 2\pi/Q$ generated by thermal motions of constituent atoms in a disordered coupled-molecular system (soft matter). Low energy phonon-like collective excitations have been observed in various biological macromolecular assemblies. In 1D liquid-crystalline DNA,[1] the effect on damping and propagation of phonons along the DNA axial direction provides evidence of a strong coupling of internal dynamics of DNA molecules and counter-ions in the surrounding solvent; in 2D lipid bilayers,[2] it is shown that the excitation softening behavior may be related to the transport of small molecules across membranes; while in 3D finite size protein systems, two globular proteins with distinct shapes and sizes, lysozyme and bovine serum albumin, show a common behavior of uniform phonon energy softening above the observed dynamic transition temperature of about T_D = 220 K.[3] Despite the finite size of proteins, low Q acoustic phonons still exist. For example, recently in electron-carrying protein cytochrome c, longitudinal sound velocity is extracted.[4] However, phonons in low-Q range are insensitive to temperature variation,[3,4] indicating that low-Q phonons do not contribute to biological function. This is because the biological activity of proteins is directly controlled by the dynamic transition temperature T_D: hydrated proteins are conformationally flexible and enzymatically active above T_D, while becoming conformationally rigid and biologically inactive below T_D.[5–8] By using inelastic X-ray scattering (IXS) technique, the phonon dispersion relation[4] as well as damping constants[3] have been extracted from measured Rayleigh-Brillouin spectra using a damped harmonic oscillator (DHO) model analysis. However, the DHO model contains no information about the central peak (Rayleigh scattering) linewidth.

The DHO model[9,10] is a simplified theory to describe approximately the phonon energy and damping in soft matter. Phonon propagation in crystals can simply be described as the characteristic harmonic oscillations of site atoms in a crystalline material. Similarly, in a soft matter system, because the relative coordinates between particles are not periodically arranged as that in crystal, the phonon propagation will be heavily damped by the non-periodicity of molecular units and anharmonic nature of the coupling between those units.

In this paper, we measure phonon dispersion relations in two hydrated proteins mainly differing for the amount of tertiary structure. One is α-chymotrypsinogen A (CHT) that presents both secondary and tertiary structural arrangements, and is the precursor of pancreas digestive enzyme α-chymotrypsin. The other is casein (Csn), the major protein in mammalian milk, which lacks tertiary structure.[11,12] From a functional point of view, Csn is recognized to be part of the milk transport system (mainly accounting for calcium and phosphate transport), and presumably influences the intestinal absorption of calcium and regulates the mineralization process of certain calcified tissues.[12] In this study, we find that phonon modes with different wavelengths have different temperature responses, indicating that only excitations with certain wavelengths are softened when temperature goes above T_D. These phonons are affected by the change in the protein mobility and might be connected to their biological activity. We also notice that the phonon population in Csn is no less than that in CHT, indicating that phonons are not propagating among different components within the tertiary structure, *i.e.* phonon population is little affected by the presence of the tertiary structure. Otherwise, casein would have much less phonon population. Therefore, the energy softening behavior happens to those phonons in the Q range lying well in the spatial scale of the secondary structure. In particular, CHT and Csn have very different β-sheet and similar α-helix abundances. The similarity of their phonon population factors

[a]*Department of Nuclear Science and Engineering, Massachusetts Institute of Technology, Cambridge, MA, 02139, USA. E-mail: sowhsin@mit.edu*
[b]*Department of Chemistry and CSGI, University of Florence, Sesto Fiorentino, Florence, I-50019, Italy*
[c]*Advanced Photon Source, Argonne National Lab, Argonne, Illinois, 60439, USA*

further implies that phonons in proteins are more likely to propagate along their individual α-helix domains within the secondary structure.

We use Generalized Three Effective Eigenmode (GTEE) theory to extract phonon energy, damping constants and central peak width (quasi-elastic linewidth) from a measured spectrum at each Q value. GTEE is aimed to deal with phonons, which are quasi-harmonic with some damping constant. Recent studies also show attempts with explicitly anharmonic models.[13,14] Due to the small vibrational amplitudes and small thermal coefficient, we believe that a harmonic description, say GTEE, is sufficient. Compared with the traditional DHO analysis of energy-shifted Brillouin peaks, GTEE not only improves the fitting quality of the overall spectrum, but it is also capable of extracting the width of the central Rayleigh peak. So far as we know, this is the first time that the GTEE theory is used to analyze the entire Rayleigh-Brillouin spectra in hydrated protein powders.

The experiments were performed with a high-energy resolution inelastic X-ray scattering beamline, 3-ID-XOR, at Advanced Photon Source (APS), Argonne National Laboratory.[15,16] High-energy resolution inline monochromator is coupled with four analyzers each separated by $\Delta Q = 3.3$ nm^{-1} in backscattering geometry. The maximum accessible Q range is up to 34 nm^{-1}.

The energy resolution function $R(E)$ of the instrument can be well described by an analytical form in terms of the following Pseudo-Voigt function,

$$R(E) = I_0\left\{2\eta/\pi\Gamma\left[1+(E/\Gamma)^2\right]^{-1} + (1-\eta)2/\Gamma(\ln 2/\pi)^{1/2}e^{-4\ln 2(E/\Gamma)^2}\right\},$$

in which η is a dimensionless parameter to adjust the mixing ratio of Lorentz-like peak and Gaussian peak, ranging from 0.41 to 0.51, while instrumental energy resolution Γ is the FWHM for both peaks, which takes value from 2.1 to 2.4 meV. Both parameter values vary among the four analyzers.

After the high-energy resolution monochromator, the beam is focused by a toroidal mirror. We have used 100 × 200 μm^2 (H × V) beam size with a photon flux of about 4.3 × 10^9 photon s^{-1} at the sample position.

α-Chymotrypsinogen A (Cat. num. C4879) and Casein (Cat. num. C7078) were purchased from Sigma-Aldrich (Milan) and used as received. The samples are prepared in the form of powder at hydration level $h = 0.33$ g g^{-1} for CHT and $h = 0.34$ g g^{-1} for Csn. In order to increase the scattering intensity, we used a rectangular sample holder with a path length of 15 mm, leading to about 20% absorption. CHT is a globular protein with $a \times b \times c = 43.83$ Å × 77.51 Å × 62.77 Å (Fig. 1), while the structure of Csn is still not completely assessed. The Csn is composed of four sub-units primarily varying in the molecular weight (from 19 000 to 25 000 Da), isoelectric point and phosphorylation level. Considering the relative abundance of proline residues and the lack of disulfide bridges, Csn has a relatively poor tertiary structure. The structure factor $S(Q)$ of CHT is reported in Fig. 2 as a function of temperature. A similar shape at high Q values (20–30 nm^{-1}) ensures that the different phonon excitation energies at different temperatures are not caused by any structural change.

de Schepper and Cohen[17] formulated a theory to calculate the dynamic structure factor based on three Q-extended hydrodynamic modes (number density, momentum density and energy density or equivalently the temperature) in simple liquids, which is called the Three Effective Eigenmode (TEE) theory. Later on in 2001, Chen and

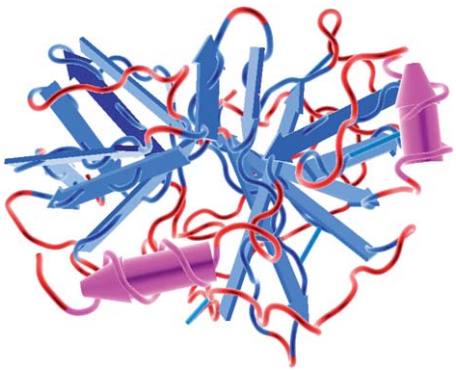

Fig. 1 3D structure of α-chymotrypsinogen A. β-sheets are denoted by blue arrows, α-helices are denoted by pink cylinders, while turns are shown in red.

Liao[18] generalized it to the case of molecular liquids, which contain multi-species of atoms, and successfully applied it to the studies of hydrated lipid bilayers[2] and liquid crystalline DNA solutions[1] by IXS. Here "generalized" means the generalization from simple liquid to polyatomic molecular liquid. GTEE is a theory, which is capable to extract transport parameters from a Rayleigh-Brillouin spectrum measured at finite Q value, well beyond the hydrodynamic limit.

According to the theory, the time evolution of correlation functions[19] among the three generalized hydrodynamic modes satisfies three by three matrix eqn (1), with the first element denoting the microscopic density fluctuation mode (n), the second element denoting the momentum density fluctuation mode (u) and the third element denoting the temperature fluctuation mode (T), respectively.[16] Essentially, GTEE theory finds the solution of the following matrix equation for the correlation function matrix $\overleftrightarrow{F}_{3\times3}(Q,z)$ among the three physical quantities:

$$z\overleftrightarrow{F}_{3\times3}(Q,z) = -\overleftrightarrow{H}(Q)_{3\times3}\overleftrightarrow{F}_{3\times3}(Q,z) + \overleftrightarrow{I}_{3\times3} \quad (1)$$

in which the generalized hydrodynamic matrix is given by

$$\overleftrightarrow{H}(Q) = \begin{pmatrix} 0 & if_{un}(Q) & 0 \\ if_{un}(Q) & z_u(Q) & if_{uT}(Q) \\ 0 & if_{uT}(Q) & z_T(Q) \end{pmatrix} \quad (2)$$

In this matrix, $f_{un}(Q)$ and $f_{uT}(Q)$ are coupling constants between different modes while $z_u(Q)$ and $z_T(Q)$ are decay rates of the corresponding modes.

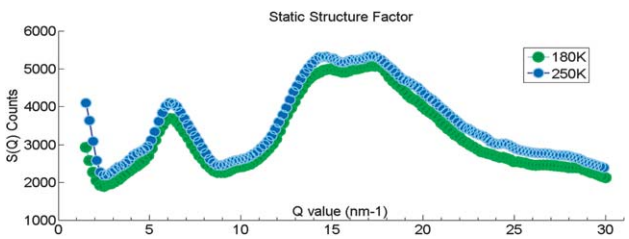

Fig. 2 Static structure factor $S(Q)$ of CHT in all Q range at 180 K and 250 K. At high Q range, S(Q) has a similar decreasing feature at 180 K and 250 K, while the phonon excitation patterns are quite distinct, indicating that the different phonon dispersion relations above and below the dynamic transition temperature are not caused by any structural change.

The inverse Laplace transform of the 1–1 element of the 3 × 3 matrix $\overleftrightarrow{F}_{3\times3}(Q,z)$ is the dynamic structure factor $S_{\mathrm{GTEE}}(Q,\omega)$, for which the normalized dynamic structure factor can be written as:

$$\frac{S(Q,\omega)_{\mathrm{GTEE}}}{S(Q)} = \frac{1}{\pi}\mathrm{Re}\left(\frac{\overleftrightarrow{I}}{z\overleftrightarrow{I}+\overleftrightarrow{H}(Q)}\right)_{1,1,z=i\omega} = \frac{1}{\pi}\mathrm{Re}\left(\frac{(z+z_u(Q))(z+z_T(Q))-(if_{uT}(Q))^2}{z^3+(z_u+z_T)z^2+\left(z_uz_T+f_{uT}^2+f_{un}^2\right)z+f_{un}^2z_T}\right) \quad (3)$$

One can define the existence of a phonon (in the parameter regime) when the third-order polynomial in the denominator of the right hand side of eqn (3) has one real and two complex conjugate roots. If the denominator has three real roots, no phonon exists. If we denote the real root as $-\Gamma_h$ and the two complex roots as $-\Gamma_s \pm i\Omega_s$, eqn (3) can be further simplified as:

$$\frac{S(Q,\omega)_{\mathrm{GTEE}}}{S(Q)} = \frac{1}{\pi}\mathrm{Re}\left(\frac{M(z)}{(z+\Gamma_h)(z+\Gamma_s-i\Omega_s)(z+\Gamma_s+i\Omega_s)}\right) = \frac{1}{\pi}\left\{A_0\frac{\Gamma_h}{\omega^2+\Gamma_h^2}+A_s\frac{\Gamma_s+b(\omega+\Omega_s)}{(\omega+\Omega_s)^2+\Gamma_s^2}+A_s\frac{\Gamma_s-b(\omega-\Omega_s)}{(\omega-\Omega_s)^2+\Gamma_s^2}\right\} \quad (4)$$

where $z = i\omega$, $M(z) = z^2 - (z_u + z_T)z + z_uz_T + f_{uT}^2$, $N = M(\Gamma_s - i\Omega_s)/[2i\Omega_s(\Gamma_h - \Gamma_s + i\Omega_s)]$ $b = -Im(N)/Re(N)$. $A_0 = M(\Gamma_h)/[(\Gamma_s - \Gamma_h)^2 + \Omega_s^2]$ is the amplitude of quasi-elastic scattering, while $A_s = Re(N)$ is the amplitude of side peaks, which is proportional to the populations of phonons.[1] Γ_h and Γ_s denote the damping constant of the heat mode (Rayleigh scattering) and the sound modes (Brillouin scattering), respectively, while Ω_s is the excitation energy of phonons.

Finally, the normalized dynamic structure factor shown in eqn (4) exhibits one central Lorentzian peak, which denotes quasi-elastic scattering, and two symmetric inelastic Lorentzian peaks, which represent the phonon creation (Stokes peak) and the phonon annihilation (anti-Stokes peak), respectively. When the coupling constant $f_{uT}(Q)$ is set to zero, *i.e.* the momentum mode decouples with the temperature mode, GTEE theory reduces to the DHO model. Thus the DHO model contains two side peaks with a vanishing central peak.[20] Since the central peak denotes the quasi-elastic scattering coming from the heat diffusion, good fitting of DHO implies that the behavior of liquid is close to the visco-elastic limit.[21] In any case, GTEE can be regarded as a generalization of the traditional DHO model for the analysis of IXS spectra. From the perspective that GTEE can be reduced to a DHO model, we can apply GTEE theory not only to molecular liquid, but also in the areas where the DHO model is not valid, such as glassy liquids or hydrated proteins.

In using GTEE theory, $I(Q,E) \propto S_{\mathrm{GTEE}}(Q,E \equiv \hbar\omega) \otimes R(E)$ *i.e.* the measured spectral intensity is not simply proportional to $S_{\mathrm{GTEE}}(Q,E)$, but to the convolution of $S_{\mathrm{GTEE}}(Q,E)$ with the energy resolution function.

In a real experiment, the measured intensity is asymmetric with the Stokes peak being higher than the anti-Stokes one, *i.e.* $S_{\mathrm{measured}}(Q,E) = e^{E/2k_BT}S_{\mathrm{GTEE}}(Q,E)$, because quantum mechanical effects have to be taken into account. This asymmetry arises in the form of the detailed balance factor $e^{E/2k_BT}$, since the measured dynamic structure factor has to satisfy the fluctuation-dissipation theorem.[22]

The Rayleigh-Brillouin spectra of both proteins are measured in the Q range from 20 nm^{-1} to 33 nm^{-1}. Low Q range excitations are not measured because previous studies[3,4] already showed that the collective excitations in the low-Q range (2–15 nm^{-1}) are temperature insensitive and not related to biological activity in proteins. Therefore, we will discuss the correlation between collective excitation energy and population, and their possible implication with the biological activity in the Q range from 20 nm^{-1} to 33 nm^{-1}. Actually, with an energy resolution of about 2.2 meV, GTEE theory is only capable of extracting well-defined phonons in the Q range about 20–33 nm^{-1}, and obtains no meaningful phonons in lower Q values, *i.e.* the denominator in eqn (3) has three real roots, as mentioned in the previous section. However, use of the DHO model allowed for the identification of low Q phonons.[3,4]

Fig. 3 shows the typical level of agreement with GTEE theory analysis of spectra taken from CHT and Csn at $Q = 29.3$ nm^{-1} and $Q = 27.9$ nm^{-1}, at all three investigated temperatures, respectively. These two Q values are chosen inside the "valley" regime of phonon dispersion relation (see Fig.4). Within this valley region, where the softening of phonons occurs, the phonon energy at and below T_D is similar, while it is markedly softened when temperature goes above T_D.

Fig. 4 shows the high Q part of the phonon dispersion relation in CHT and Csn, at 180 K (below T_D), 220 K (about T_D) and 250 K (above T_D), respectively. Taking into account the length scale of α-helices and β-sheets, which is about 5 Å for the pitch of α-helix and about 7.5 Å of pleat length of β-sheet, we infer that phonons mainly propagate within the typical length scale existing in the secondary structure.

In both proteins, we can see that phonon energies are softened from about 26 to about 30 nm^{-1}, which take the shape of a valley. In the investigated temperature range, the valley corresponds to a spatial distance of about $2\pi/Q_{\mathrm{min}}\sim2.2$ Å. Within this Q range, the excitation energies at 180 K and 220 K are almost the same, while they markedly soften as the temperature increases above T_D, at 250 K.

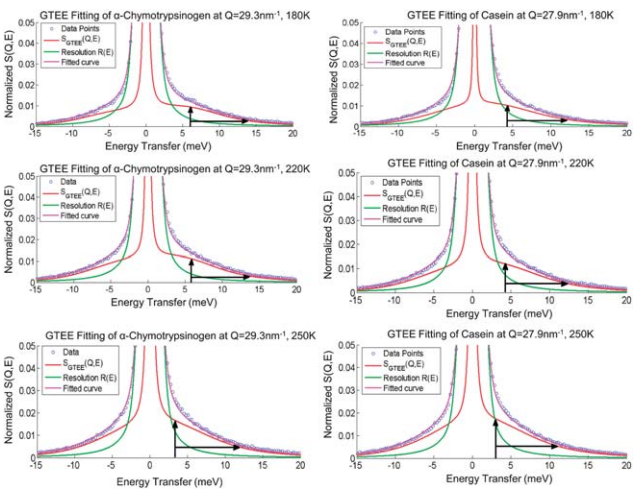

Fig. 3 Typical analysis results using GTEE theory. Resolution function $R(E)$ (green line), when it convolutes with theoretical $S_{\mathrm{GTEE}}(Q,E)/S(Q)$ (red line), gives the purple line, which can be directly compared with experimental data (circular dots). The vertical arrows denote phonon energies while horizontal arrows denote phonon damping constants. We can easily see that phonon energies are softened above $T_D = 220$ K, *i.e.* the vertical line shifts to the left at 250 K in both proteins. From the increased level of the skirt of $S_{\mathrm{GTEE}}(Q,E)/S(Q)$, we also see the characteristic feature that phonon population increases with temperature.

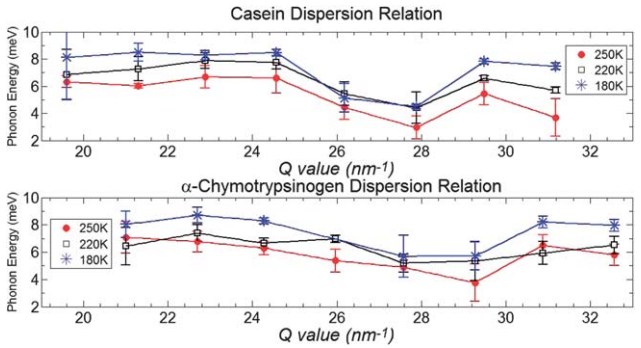

Fig. 4 Measured phonon dispersion relation in high Q range. Phonon energies are gradually lowered as temperature is raised in the whole Q range from 20 nm^{-1} to 31 nm^{-1}. But note, in particular, within a narrow Q range from 27 nm^{-1} to 31 nm^{-1} for CHT, and from 24 nm^{-1} to 30 nm^{-1} for Csn, phonons are markedly softened compared with other Q values, which form a valley within the dispersion relation. At the bottom of this valley (Q ≈ 28 to 29 nm^{-1}), the phonon energies are similar at 180 K and 220 K, but suddenly drop down above 220 K. Since proteins are biologically active above 220 K,[5–8] this indicates that phonon softening might be related to the onset of biological activity.

This temperature effect is related to the crossover temperature of hydration water of the proteins.[23,24] Previous experiments show that the hydration water of biological macromolecules exhibits a dynamic crossover at about 220 K, where its temperature dependence measured by quasi-elastic neutron scattering undergoes to a profound change.[25–27] It was suggested that this dynamic crossover of hydration water is closely related to the dynamic transition of the bio-molecules themselves while crossing the Widom line in the liquid phase region.[28] Therefore, we can figure out that phonons with wavelength within this Q range are contributing both to the protein dynamics and activity. At $Q \approx 28$ to 29 nm^{-1}, the dispersion relations of the two proteins show a common bottom of the valley. Moreover, the temperature sensitivity of phonon energies is different at Q values outside the valley. For instance, at $Q > 30$ nm^{-1}, the phonon energies drop down as temperature increases to 220 K, indicating the existence of a certain degree of freedom triggered by the temperature increment. We speculate that the phonon excitation softening above the dynamic transition temperature might contribute to the onset of the protein biological functions.

Unlike the existence of a well-defined valley in the phonon dispersion relation, the damping constants of CHT and Csn have an increasing trend as temperature and Q value increase (see Fig. 5). This feature is quite reasonable, since phonon population will increase as temperature goes up (see Fig. 8), leading to a higher probability of phonon–phonon interaction. Larger phonon–phonon interaction will cause a greater damping of phonons. As temperature increases the oscillatory behavior of the phonon damping decreases. At 250 K, the damping is almost linear above $Q > 23$ nm^{-1}. This behavior is in agreement with that of simple liquids, for which the damping increases monotonously with Q.[21] Actually, proteins are glassy below T_D at 180 K, while above T_D, at 250 K, proteins are liquid-like.

Fig.6 shows the intermediate scattering function (ISF) of CHT at $Q = 24.3$ nm^{-1}. ISF is the frequency-time Fourier transform to the dynamic structure factor (eqn (4)).[19,21] Firstly, it shows a two-step relaxation, with characteristic times $2\pi/\Gamma_s$ and $2\pi/\Gamma_h$, respectively. Secondly, there is small upturn around the kink between the two relaxations, which is originated from the phonon oscillation. Thirdly,

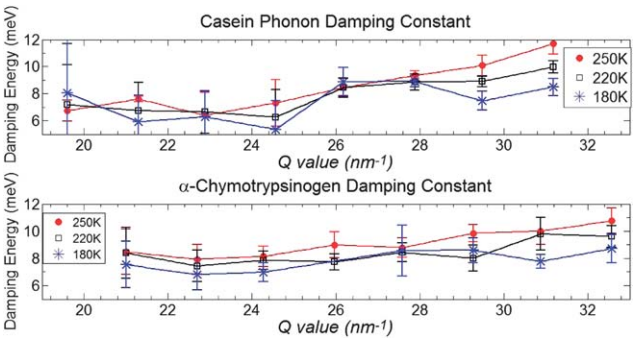

Fig. 5 Measured phonon damping constant Γ_s for CHT and Csn, at all three investigated temperatures. The damping curve oscillates at 180 K, while it becomes smoother when temperature increases.

the phonon contribution (the amplitude of the dot-dashed line at short time) increases with temperature, indicating the increase of conformational flexibility.

Most importantly, we are able to extract the central peak width with high accuracy without using eqn (4) by working in the Fourier transformed space. In this regard, we can avoid the cumbersome convolution operation, which increases the fitting error, and the fitting can be easily performed with one single exponential function. By using convolution theorem and Fourier transform, we get:

$$S_{\text{measured}}(Q,\omega) = S_{\text{GTEE}}(Q,\omega) \otimes R(E)$$
$$\Rightarrow FT\{S_{\text{measured}}(Q,E)\} = F_{\text{GTEE}}(Q,t) \times FT\{R(E)\} \quad (5)$$

where

$$F_{\text{GTEE}}(Q,t) = A_0 e^{-\Gamma_h t} + (1 - A_0) e^{-\Gamma_s t}(\cos \Omega_s t + b \sin \Omega_s t) \quad (6)$$

and FT denotes Fourier transform.

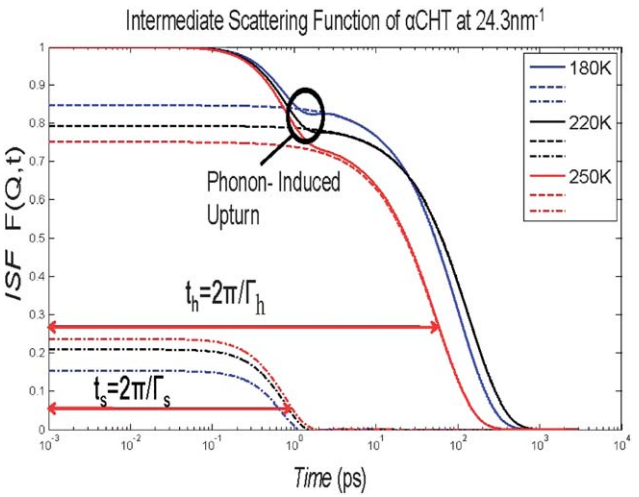

Fig. 6 Intermediate scattering function of CHT at $Q = 24.3$ nm^{-1} and at the three measured temperatures. This figure illustrates the characteristic two-step relaxation in protein dynamics up to 1 ns. The dashed lines, which overlap with the ISF over a long time, are the quasi-elastic (Rayleigh Peak) contribution, while the lower dot-dashed lines are the contribution of phonon part; the sum of the two parts is exactly the ISF. At longer times, the contribution of sound mode vanishes, leaving a long time relaxation which gives an accurate value of the central peak width, Γ_h.

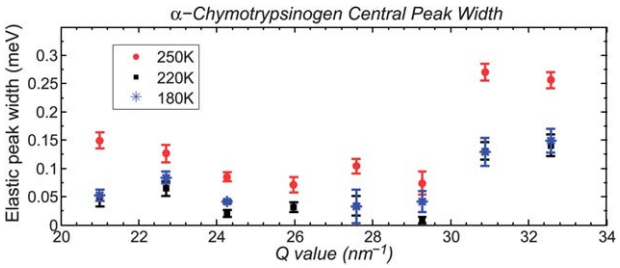

Fig. 7 Central Rayleigh peak widths (generalized heat diffusion mode) Γ_h of CHT at the three measured temperatures. At 180 K and 220 K, the widths differ not much with each other; the difference becomes apparent only above T_D, at 250 K. Unlike phonon excitation energy, such phenomena occur at all Q ranges. The peak width shows a decreased relaxation time above T_D. The typical order of Γ_h is about 0.1 meV, which is much smaller than the instrumental resolution of 2.2 meV. We are able to extract this parameter having magnitude much smaller than resolution only by analysis of ISF in the time domain using GTEE theory.

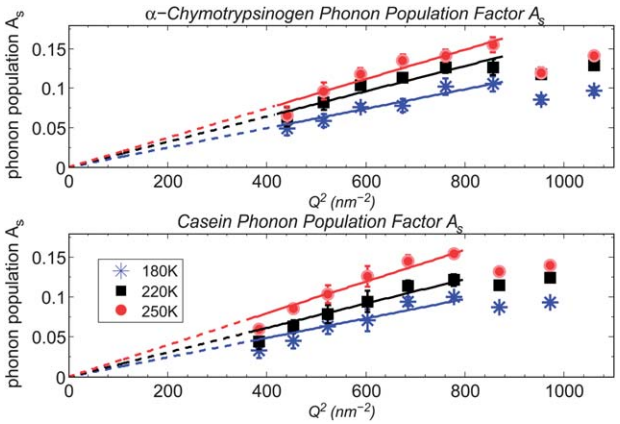

Fig. 8 The fractional amplitude of the phonon mode A_s in CHT and Csn. The slope is proportional to $\langle x^2 \rangle$, indicating an increase of $\langle x^2 \rangle$ as temperature goes up. When Q increases, the phonon peak amplitudes also increase according to Q^2 relation, except for a very high Q range ($Q > 30$ nm^{-1}), where the low Q expansion of the Debye–Waller factor is no longer valid, see eqn (6).

In other words, other than fitting $S_{GTEE}(Q,E)$ in eqn (4), we fit its Fourier transform (eqn (6)) $F_{GTEE}(Q,t)$. At large t ($t > 10$ ps), the phonon contribution in $F_{GTEE}(Q,t)$ (second term in eqn (6), also the dot-dashed lines in Fig. 6) vanishes, and only the α relaxation (first term in eqn (6), dot lines in Fig. 6) contributes. In particular, the typical value of Γ_s is 100 times larger than Γ_h, which means the side-peak contribution to $F_{GTEE}(Q,t)$ decays $\sim e^{100}$ faster than α relaxation. This allows us to fit only the long time part of $F_{GTEE}(Q,t)$, which is a single exponential form, leading to a higher accuracy for Γ_h. Fig. 7 shows the finite Q heat diffusion constant Γ_h with small errorbar, from which we can see that the typical value of heat diffusion rate is 0.1 meV. Therefore, the heat diffusion rate, which cannot be extracted from the DHO model, can easily be analyzed through the Fourier transformed spectra of GTEE theory.

In order to verify the validity of the fitting, we compare the calculated phonon amplitudes A_s to a Q^2 law obtained from the Debye-Waller factor. At small Q value, the amplitude of the elastic peak A_0 is proportional to the Debye–Waller factor $\exp(-Q^2\langle x^2 \rangle)$, which indicates that the low Q expansion of $A_s = 1/2(1 - A_0)$ has a form $A_s = \alpha(T)Q^2$, where $\alpha(T)$ increases with temperature due to the increase of phonon population, associated with the higher conformational flexibility of the proteins. Fig. 8 shows A_s *vs.* Q as a function of temperature in both CHT and Csn. We can see clearly that the phonon amplitudes fit the Q^2 law very well, except for the range $Q > 30$ nm^{-1}, where the low Q expansion for Q^2 relation is no longer valid.

Fig. 8 clearly shows that the phonon amplitudes at the same Q and temperature values are similar for both proteins (from $\sim$0.04 at 20 nm^{-1} to $\sim$0.14 at 30 nm^{-1}). Csn presents a poor tertiary structural arrangement while CHT is mainly globular with a well defined tertiary structure. Considering the similar phonon behavior for the two proteins, we speculate that phonons do not rely on the presence of tertiary or quaternary structures, while secondary structures, such as α-helices and β-sheets,[29] appear to be involved in the phonons propagation. Csn protein is natural combination of Csn-α_1, Csn-α_2, Csn-β and Csn-κ, and has an average ratio of[30] 15% α-helices and 30% β-sheets, while CHT has 13% α-helices but 50% β-sheets.[31] If phonons are all propagating within the structure of β-sheets, the phonon population in CHT will be much larger than Csn. Therefore, such similar phonon population between CHT and Csn indicates that phonons are unlikely to propagate along β-sheets; α-helices are more likely to accommodate phonons in secondary structures.

Summarizing, we use GTEE theory to analyze IXS Rayleigh-Brillouin spectra in the Q range between 20 nm^{-1} and 31 nm^{-1}. We obtain the dispersion and damping of collective excitations in two structurally different proteins, α-chymotrypsinogen A and casein. We choose to perform the analysis in terms of the intermediate scattering function $F(Q,t)$ (eqn (6)) in the time domain to extract values of the central peak widths. This approach allows us to avoid complicated convolution operation, and analyze the long time behavior of $F(Q,t)$ only. As a consequence, the uncertainties of the central peak widths are strongly reduced.

We observe, especially for Csn, a "valley" in the phonon dispersion relation around $Q \sim 28$ nm^{-1}, where the softening of phonon is evident. The significance of softening at certain Q is to lower the frequency of this mode of vibration and thus gain more motional flexibility in the length scale of $2\pi/Q$. The softening becomes apparent above the dynamic transition temperature, T_D. Phonon populations obey the Q^2-law, which shows that the GTEE fitting results are accurate. The phonon population increases with temperature, which is also reasonable because of the more conformational flexibility at higher temperatures. In addition, considering the conformational differences between the two proteins, it is plausible to infer that phonon excitations are unlikely to propagate among components in the tertiary structure. The comparison of the ratio of α-helices and β-sheets between the two selected proteins implies that phonon propagation is more likely along individual α-helix domains.

Acknowledgements

This research at MIT is supported by a grant from Basic Energy Sciences Division of US DOE DE-FG02-90ER45429. The work at the Advanced Photon Source was supported by the U.S. Department of Energy, Office of Science, Office of Basic Energy Sciences, under Contract No. DE-AC02-06CH11357. Emiliano Fratini and Piero Baglioni acknowledge the financial support from Ministero dell'Istruzione, Università e della Ricerca Scientifica (MIUR, grant

PRIN-2008, prot. 20087K9A2J, and FIRB-RBPR05JH2P007 Italnanonet) and Consorzio Interuniversitario per lo Sviluppo dei Sistemi a Grande Interfase (CSGI).

References

1 Y. Liu, S.-H. Chen, D. Berti, P. Baglioni, A. Alatas, H. Sinn, E. Alp and A. Said, *J. Chem. Phys.*, 2005, **123**, 214909.
2 S. H. Chen, C. Y. Liao, H. W. Huang, T. M. Weiss, M. C. Bellissent-Funel and F. Sette, *Phys. Rev. Lett.*, 2001, **86**, 740.
3 D. Liu, X. Chu, M. Lagi, Y. Zhang, E. Fratini, P. Baglioni, A. Alatas, A. Said, E. Alp and S.-H. Chen, *Phys. Rev. Lett.*, 2008, **101**, 135501.
4 B. M. Leu, A. Alatas, H. Sinn, A. H. Said, E. E. Alp, H. Yavas, J. Zhao, J. T. Sage and W. Sturhahn, *J. Chem. Phys.*, 2010, **132**, 085103.
5 G. Zaccai, *Science*, 2000, **288**, 1604–1607.
6 B. Rasmussen, A. Stock, D. Ringe and G. Petsko, *Nature*, 1992, **357**, 423–424.
7 F. Parak, E. W. Knapp and D. Kucheida, *J. Mol. Biol.*, 1982, **161**, 177–210; B. Fåk and B. Dorner, *Phys. B*, 1997, **234–236**, 1107–1108.
8 F. Parak and K. Achterhold, *J. Phys. Chem. Solids*, 2005, **66**, 2257–2262.
9 F. Sette, G. Ruocco, M. Krisch, C. Masciovecchio, R. Verbeni and U. Bergmann, *Phys. Rev. Lett.*, 1996, **77**, 83–86.
10 B. Fåk and B. Dorner, *Phys. B*, 1997, **234–236**, 1107–1108.
11 L. Sen, H. Lee, R. Feeney and J. Whitaker, *J. Agric. Food Chem.*, 1981, **29**, 348–354.
12 D. Jenkins, K. Srichaikul, J. Wong, C. Kendall, B. Bashyam, E. Vidgen, B. Lamarche, A. Rao, P. Jones, R. Josse, C. Jackson, T. Leong and L. Leiter, *J. Nutr.*, 2010, **140**, 1633.
13 R. Granek and J. Klafter, *Phys. Rev. Lett.*, 2005, **95**, 098106.
14 S. Reuveni, R. Granek and J. Klafter, *Proc. Natl. Acad. Sci. U. S. A.*, 2010, **107**, 13696.
15 H. Sinn, E. E. Alp, A. Alatas, J. Barraza, G. Bortel, E. Burkel, D. Shu, W. Sturhahn, T. Toellner and J. Zhao, *Nucl. Instrum. Methods Phys. Res., Sect. A*, 2001, **467–468**, 1545.
16 T. Toellner, A. Alatas and A. Said, *J. Synchrotron Radiat.*, 2011, **18**, 605–611.
17 I. de Schepper, E. Cohen and C. Bruin, *Phys. Rev. A: At., Mol., Opt. Phys.*, 1988, **38**, 271–287.
18 C. Liao and S.-H. Chen, *Phys. Rev. E: Stat. Phys., Plasmas, Fluids, Relat. Interdiscip. Top.*, 2001, **64**, 021205.
19 J. P. Boon and S. Yip, *Molecular Hydrodynamics*, Dover Publications, 1992.
20 F. Sette, G. Ruocco, M. Krisch, U. Bergmann, C. Masciovecchio, V. Mazzacurati, G. Signorelli and R. Verbeni, *Phys. Rev. Lett.*, 1995, **75**, 850–853.
21 R. Crevecoeur, H. Smorenburg and I. de Schepper, *J. Low Temp. Phys.*, 1996, **105**, 149.
22 S.-H. Chen and M. Kotlarchyk, *Interactions of Photons and Neutrons with Matter*, World Scientific Publishing Co. Pte. Ltd, 2007.
23 F. G. Parak, *Rep. Prog. Phys.*, 2003, **66**, 103.
24 X. Chu, A. Faraone, C. Kim, E. Fratini, P. Baglioni, J. Leao and S.-H. Chen, *J. Phys. Chem. B*, 2009, **113**, 5001–5006.
25 S. H. Chen, L. Liu, E. Fratini, P. Baglioni, A. Faraone and E. Mamontov, *Proc. Natl. Acad. Sci. U. S. A.*, 2006, **103**, 9012–9016.
26 S. H. Chen, L. Liu, X. Chu, Y. Zhang, E. Fratini, P. Baglioni, A. Faraone and E. Mamontov, *J. Chem. Phys.*, 2006, **125**, 171103.
27 X. Q. Chu, E. Fratini, P. Baglioni, A. Faraone and S. H. Chen, *Phys. Rev. E: Stat., Nonlinear, Soft Matter Phys.*, 2008, **77**, 011908.
28 P. H. Poole, F. Sciortino, U. Essmann and H. E. Stanley, *Nature*, 1992, **360**, 324–328.
29 L. Pauling and R. B. Corey, *Proc. Natl. Acad. Sci. U. S. A.*, 1951, **37**, 251–256.
30 D. S. Horne, *Curr. Opin. Colloid Interface Sci.*, 2002, **7**, 456–461.
31 D. Byler and H. Susi, *Biopolymers*, 1986, **25**, 469–487.

